

distance from the competitor. Therefore, we presume that the strength or extent of the short-range destabilizing signals increases during synaptic maturation [as synaptic efficacy is increasing (11)] or that the destabilization process is itself incremental (taking longer to remove distant synapses than nearby ones), or that both processes occur. Because the decreasing signals may become totally ineffective when the competitors are sufficiently separated (17), the normal confinement of all the incoming axons to a small AChR plaque may thus be a strategy that encourages strong competition among nearby synapses, which rapidly results in single innervation at developing neuromuscular junctions. Given the existence of competitive synaptic reorganization on neurons (18) and the evidence for the restriction of axonal innervation to parts of a dendritic arbor (19), it seems likely that analogous short-range signals operate throughout the nervous system.

References and Notes

1. D. Purves and J. W. Lichtman, *Principles of Neural Development* (Sinauer, Sunderland, MA, 1985).
2. P. A. Redfern, *J. Physiol.* **209**, 701 (1970); J. K. S. Jansen and T. Fladby, *Prog. Neurobiol.* **34**, 39 (1990).
3. W.-B. Gan and E. R. Macagno, *J. Neurosci.* **15**, 3243 (1995).
4. Neonatal mice (between P0 and P17) were anesthetized with 0.1 ml of sodium pentobarbital. Sternomastoid muscles were then dissected and placed in petri dishes in physiological saline. In some cases, junctional AChRs were labeled for 10 min with tetramethyl rhodamine-conjugated α -bungarotoxin (5 μ g/ml) (Molecular Probes, Eugene, OR). Sharp electrodes (5 to 10 megohms, as measured with 3 M KCl) were backfilled with a 1% solution of 3,3'-diiodoacetylcarbo-cyanine perchlorate (DiO) (Molecular Probes) in a 100% solution of methylene chloride (Sigma) and positioned on a superficial neuromuscular junction. Depolarizing current (200 ms, 1 to 10 nA, and 1 Hz) was applied for a few seconds until a dye crystal was deposited at the junction. The muscle was then fixed in a 4% solution of paraformaldehyde for 12 hours, over which time the fluorescent DiO lipid labeled many terminals of one motor unit that were distributed over several hundred micrometers. For the labeling of two competing axons at the same neuromuscular junction, two electrodes [each containing 1% solutions of either 1,1'-diiodoacetyl-3,3',3'-tetramethylindocarbocyanine perchlorate (DiI) (Molecular Probes) or DiO in a 100% solution of methylene chloride] were used to deposit dye. In this way, two different subsets of axon terminals, which by chance occasionally converged at the same junction, were labeled. All labeled junctions were imaged with confocal microscopy (Noran Odyssey, Olympus Fluoview, and Bio-Rad MRC1024) with 1.4-numerical aperture objectives, and three-dimensional (3D) reconstructions were generated with the Bio-Rad MRC1024 software.
5. R. J. Balice-Gordon and J. W. Lichtman, *J. Neurosci.* **13**, 834 (1993).
6. Staining of all motor axons [with antibodies against neurofilaments, synaptic vesicles (SV2), and acetylated microtubules] was done similarly as described in (11). For tetanus toxin labeling, the preparation was incubated with a fluorescein isothiocyanate-conjugated recombinant tetanus toxin C fragment (Boehringer Mannheim) for 20 min (1:10 dilution).
7. R. J. Balice-Gordon, C. K. Chua, C. C. Nelson, J. W. Lichtman, *Neuron* **11**, 801 (1993).
8. To measure the separation of two competing axons, we calculated a segregation index as the distance between centroids of the competing axons divided by the total length of the junction, which was measured along a line passing through the two centroids. The centroid (geometric center) of the terminal branches of each competing axon was obtained with IP Lab software (Scanalytics, Fairfax, VA). The particular shape of the junction will influence this measure to some degree. For hemicircles that approximate the shapes of competing axon terminals, values >0.39 indicate that the regions are completely segregated.
9. Because of the low incidence of multiply innervated junctions after P12, we used antibody staining instead of lipophilic dyes to label competing axons at P16-17. Competing axons innervating the same junction at this age were traced several hundred micrometers back into nerve bundles to confirm that they were separate axons.
10. D. A. Riley, *Brain Res.* **134**, 279 (1977); *J. Neurocytol.* **10**, 425 (1981).
11. H. Colman, J. Nabekura, J. W. Lichtman, *Science* **275**, 356 (1997).
12. G. S. Stent, *Proc. Natl. Acad. Sci. U.S.A.* **70**, 997 (1973).
13. R. J. Balice-Gordon and J. W. Lichtman, *Nature* **372**, 519 (1994); C. Jennings, *ibid.*, p. 498.
14. Y.-J. Lo and M.-M. Poo, *Science* **254**, 1019 (1991); Y. Dan and M.-M. Poo, *ibid.* **256**, 1570 (1992); S. Cash, Y. Dan, M.-M. Poo, R. Zucker, *Neuron* **16**, 745 (1996).
15. S. Rotzler, H. Schramek, H. R. Brenner, *Nature* **349**, 337 (1991).
16. D. J. Zou and H. T. Cline, *Neuron* **16**, 529 (1996); G.-Y. Wu, R. Malinow, H. T. Cline, *Science* **274**, 972 (1996).
17. M. C. Brown, J. K. S. Jansen, D. Van Essen, *J. Physiol.* **261**, 387 (1976); D. Kuffler, W. Thompson, J. K. S. Jansen, *Brain Res.* **138**, 353 (1977).
18. D. H. Hubel, T. N. Wiesel, S. LeVay, *Philos. Trans. R. Soc. London Ser. B* **278**, 377 (1977); D. Purves and J. W. Lichtman, *Science* **210**, 153 (1980); M. C. Crair, D. C. Gillespie, M. P. Stryker, *ibid.* **279**, 566 (1998); A. A. Penn, P. A. Riquelme, M. B. Feller, C. J. Shatz, *ibid.*, p. 2108.
19. C. J. Forehand and D. Purves, *J. Neurosci.* **4**, 1 (1984); R. Young and E. W. Rubel, *J. Comp. Neurol.* **254**, 425 (1986); M. Bank and S. Schacher, *J. Neurosci.* **12**, 2960 (1992); M. Bravin, F. Rossi, P. Strata, *J. Comp. Neurol.* **357**, 395 (1995).
20. M. M. Rich and J. W. Lichtman, *J. Neurosci.* **9**, 1781 (1989).
21. We thank all the members of our lab for helpful discussion of this work; J. R. Sanes, R. O. Wong, and M. L. Nonet for comments on the manuscript; and S. G. Turney for technical help. This work was supported by grants from NIH and the Muscular Dystrophy Association. W.-B.G. was supported by a National Research Service Award from NIH.

26 August 1998; accepted 20 October 1998

The Role of Far1p in Linking the Heterotrimeric G Protein to Polarity Establishment Proteins During Yeast Mating

Anne-Christine Butty, Peter M. Pryciak, Linda S. Huang, Ira Herskowitz, Matthias Peter*

Heterotrimeric guanosine triphosphate (GTP)-binding proteins (G proteins) determine tissue and cell polarity in a variety of organisms. In yeast, cells orient polarized growth toward the mating partner along a pheromone gradient by a mechanism that requires Far1p and Cdc24p. Far1p bound G $\beta\gamma$ and interacted with polarity establishment proteins, which organize the actin cytoskeleton. Cells containing mutated Far1p unable to bind G $\beta\gamma$ or polarity establishment proteins were defective for orienting growth toward their mating partner. In response to pheromones, Far1p moves from the nucleus to the cytoplasm. Thus, Far1p functions as an adaptor that recruits polarity establishment proteins to the site of extracellular signaling marked by G $\beta\gamma$ to polarize assembly of the cytoskeleton in a morphogenetic gradient.

Asymmetric cellular organization or cell polarity is a central feature of morphogenesis and is controlled by both internal and external signals (1). In the yeast *Saccharomyces cerevisiae*, mating pheromones trigger a mitogen-activated

protein kinase (MAPK) signal transduction pathway, culminating in arrest of the cell cycle, changes in gene expression, and altered cell polarity and morphology (2). These responses are initiated by a cell-surface receptor coupled to a G protein. Activation of the pheromone receptor triggers dissociation of the heterotrimeric G protein into subunits G α and G $\beta\gamma$, which in turn signal to downstream effectors to induce cellular responses (3). Cells use a pheromone gradient to locate their mating partner and polarize their actin cytoskeleton toward the site of the highest pheromone concentration (4). Far1p and Cdc24p are necessary for oriented cell polarity: specific alleles of *FAR1* (*far1-s*) and *CDC24* (*cdc24-m*) have been identified which cause a specific mating defect, because

A.-C. Butty and M. Peter, Swiss Institute for Experimental Cancer Research (ISREC), Chemin des Boveresses 155, 1066 Epalinges/VD, Switzerland. P. M. Pryciak, Department of Molecular Genetics and Microbiology, University of Massachusetts Medical Center, Worcester Foundation Campus, 222 Maple Avenue, Shrewsbury, MA 01545, USA. L. S. Huang and I. Herskowitz, Department of Biochemistry and Biophysics, University of California, San Francisco, San Francisco, CA 94143-0448, USA.

*To whom correspondence should be addressed. E-mail: matthias.peter@isrec.unil.ch

REPORTS

these cells are unable to locate their mating partner (5, 6). Genetic experiments also implicate the G protein in the regulation of cell polarity during mating (7).

Morphological changes during mating depend on reorganization of the actin cytoskeleton by a group of proteins including Cdc24p, Bem1p, Cdc42p, and the two Gic proteins (Gic1p and Gic2p) that are necessary for establishment of cell polarity (1, 8). Cdc24p functions as a GDP-GTP exchange factor (GEF) for Cdc42p (9), whereas the Gic proteins are effectors of Cdc42p involved in organizing the actin cytoskeleton (8). Bem1p contains two SH3 domains and interacts with Cdc42p, Cdc24p, Ste20p, Far1p and, Ste5p (10–13). Bem1p co-immunoprecipitates with actin (12), suggesting that it is involved in recruiting the actin cytoskeleton to the site of polarization. Little is known about how the polarity establishment proteins are targeted to the site of polarization.

To examine the role of Far1p in orienting polarized growth during mating, we tested by two-hybrid analysis whether Far1p was able to interact with the polarity establishment

proteins Bem1p, Cdc42p, Cdc24p, and Gic2p (14, 15). Far1p interacted with Bem1p, Cdc24p, and Cdc42p but not with Gic2p or a truncated Cdc24p, which lacks a portion of the NH₂-terminal domain (Table 1). Far1p was unable to interact with the guanosine triphosphatase (GTPase) Rho1p, demonstrating that Cdc42p is a specific GTPase-binding partner of Far1p. Far1p preferentially bound to Cdc42p in its active GTP-bound state, whereas little binding was observed when Cdc42p was bound to guanosine diphosphate (GDP). Because Bem1p also interacted with Cdc42p in a GTP-dependent manner (Table 1) (10, 11), we tested whether the interaction between Far1p and Cdc42p-GTP was dependent on the presence of Bem1p. The interaction between Cdc42p and Far1p was abolished in a strain deleted for *BEM1*, whereas Cdc24p was able to interact with Far1p under these conditions (Table 1). Thus, Far1p interacts with the polarity establishment proteins Bem1p and Cdc24p, and Bem1p may bridge the interaction between Far1p and Cdc42p-GTP.

To examine whether Bem1p could directly bind to Far1p in vitro, Far1p was fused to its NH₂-terminus to two copies of the polyoma epitope (PT-Far1p) and purified from yeast (16). Cells expressing a hemagglutinin (HA) epitope-tagged version of Far1p (HA-Far1p) were used as a control. PT-Far1p was immobilized on a polyoma antibody affinity column and probed with Bem1p expressed as a 6His protein in *Escherichia coli*. After extensive washing, Far1 protein was eluted using polyoma-peptide, and bound Bem1p was detected by immunoblotting. Bem1p readily bound to the PT-Far1p column (Fig. 1A), whereas no binding was detected with HA-Far1p, demonstrating that Far1p and Bem1p interact specifically in vitro. Treating the cells expressing PT-Far1p with α factor did not alter the efficiency of binding between Far1p and Bem1p, suggesting that the interaction between Far1p and Bem1p was not modified by pheromone induction (13, 15). Coimmunoprecipitation experiments also confirmed that Far1p interacted with Cdc24p in vivo: cells expressing epitope-tagged Cdc24p (HA-Cdc24p) or control cells expressing untagged Cdc24p were treated with α factor, and then HA-Cdc24p was precipitated with HA11 antibodies and analyzed for the presence of Far1p expressed from the inducible *GAL* promoter by immunoblotting (17). Far1p readily coprecipitated with Cdc24p (Fig. 1B), demonstrating that Far1p bound to Cdc24p in vivo.

To determine whether Far1p might be an effector of G $\beta\gamma$, we next tested the ability of Far1p to coprecipitate with Ste4p, the β subunit of the yeast heterotrimeric G protein (Fig. 1C). Far1p was readily detectable in HA11 immunoprecipitates from cells expressing epitope-tagged Ste4p (HA-Ste4p) but not in immunoprecipitates from control cells expressing untagged Ste4p. In addition, a specific interaction between Far1p and Ste4p was detected by two-hybrid analysis (Table 1 and Fig. 2A). Because expression of Ste4p activates the pheromone response pathway, these experiments do not address whether the interaction between Far1p and Ste4p is regulated by pheromones. However, G $\beta\gamma$ bound to Far1p and could use Far1p to orient the cytoskeleton toward the mating partner.

Cdc24p interacts with Ste4p (6, 18), and mutants of Cdc24p have been identified which fail to interact with G $\beta\gamma$ (6). The interaction of Cdc24p and Ste4p in vivo is likely to depend on Far1p. First, the interaction between Cdc24p and Ste4p assessed by the two-hybrid system was abolished in strains deleted for *FAR1* (Fig. 1D). Second, Far1p interacted independently with both Cdc24p and Ste4p (Table 1 and Fig. 2), and Cdc24 mutant proteins that were unable to interact with Ste4p (6, 18) were all unable to

Table 1. Two-hybrid interactions among Far1p, Bem1p, Cdc24p, Cdc42p, Rho1p, and Ste4p in wild-type cells (EGY48) or derivatives deleted for *BEM1* or *STE7*. The activation domain fusions were carried on pJG4-5-based vectors; the LexA DNA-binding domain fusions were carried on pEG202-based vectors (14). Miller units with standard deviations are presented; assays were done as described (15).

Activation domain fusion	DNA-binding domain fusion	Miller units \pm SD
<i>EGY48</i>		
Far1p (1–830)	Bem1p	780 \pm 254
Vector	Bem1p	23 \pm 25
Far1p (1–830)	Cdc42 ^{C188S} p	840 \pm 205
Vector	Cdc42 ^{C188S} p	65 \pm 59
Far1p (1–830)	Rho1p ^{C206S}	8 \pm 1
Vector	Rho1p ^{C206S}	13 \pm 6
Far1p (1–830)	Cdc42 ^{C188S} p(G12V) GTP bound	1032 \pm 397
Far1p (1–830)	Cdc42 ^{C188S} p(D118A) GDP bound	3 \pm 1
Vector	Cdc42 ^{C188S} p(G12V) GTP bound	154 \pm 13
Cdc42 ^{C188S} p	Bem1p	348 \pm 93
Cdc42 ^{C188S} p(G12V) GTP bound	Bem1p	1009 \pm 278
Cdc42 ^{C188S} p(D118A) GDP bound	Bem1p	31 \pm 5
Far1p (1–830)	Cdc24p	1688 \pm 118
Vector	Cdc24p	58 \pm 7
Far1p (1–830)	Cdc24p- Δ N	6 \pm 4
Far1p (1–830)	Cdc24p-m1	4 \pm 2
Far1p (1–830)	Cdc24p-m2	12 \pm 4
Far1p (1–830)	Cdc24p-m3	8 \pm 3
Ste4p	Cdc24p	471 \pm 39
Ste4p	Vector	3
Ste4p	Cdc24p- Δ N	3 \pm 2
Ste4p	Cdc24p-m1	8 \pm 3
Ste4p	Cdc24p-m2	14 \pm 5
Ste4p	Cdc24p-m3	12 \pm 3
<i>EGY48 Δste7</i>		
Far1p (1–830)	Ste4p	1493 \pm 100
Vector	Ste4p	235 \pm 172
<i>EGY48 Δbem1</i>		
Far1p (1–830)	Bem1p	1170 \pm 379
Far1p (1–830)	Cdc24p	1532 \pm 105
Far1p (1–830)	Cdc42 ^{C188S} p	23 \pm 20
Gic2p	Cdc42 ^{C188S} p	3840 \pm 189
Vector	Bem1p	8 \pm 1
Vector	Cdc42 ^{C188S} p	23 \pm 21
Vector	Cdc24p	102 \pm 57

REPORTS

bind Far1p (Table 1), indicating that the domain of Cdc24p that mediated interaction with Far1p was also required for the interaction with Ste4p. Finally, genetic analysis indicated that *cdc24-m* and *far1-s* mutants are defective in the same pathway (Fig. 1E) (19). Thus, Far1p is needed to bridge the interaction between Gβγ and the polarity establishment proteins in vivo.

To address the functional importance of the interaction between Far1p, Gβγ, and the polarity establishment proteins, we tested whether any of the mutant Far1 proteins unable to orient polarization in vivo (5) failed to interact with Bem1p, Cdc42p, Cdc24p, or Ste4p (Fig. 2) (20). Far1p¹⁻³⁸⁹, which lacked the COOH-terminal half of the protein, was defective for interacting with Bem1p, Cdc24p, and Cdc42p, although it was able to bind Ste4p. Similarly, the Far1p-H7 mutation (5) was unable to bind to Bem1p and Cdc42p and exhibited strongly reduced binding to Cdc24p, but still allowed efficient interaction with Gβγ (Fig. 2). Analysis of additional Far1p mutants indicated that the RING finger domain of Far1p was necessary and sufficient for interaction with Gβγ. Mutants lacking all or part of the RING finger domain were unable to form oriented mating projections,

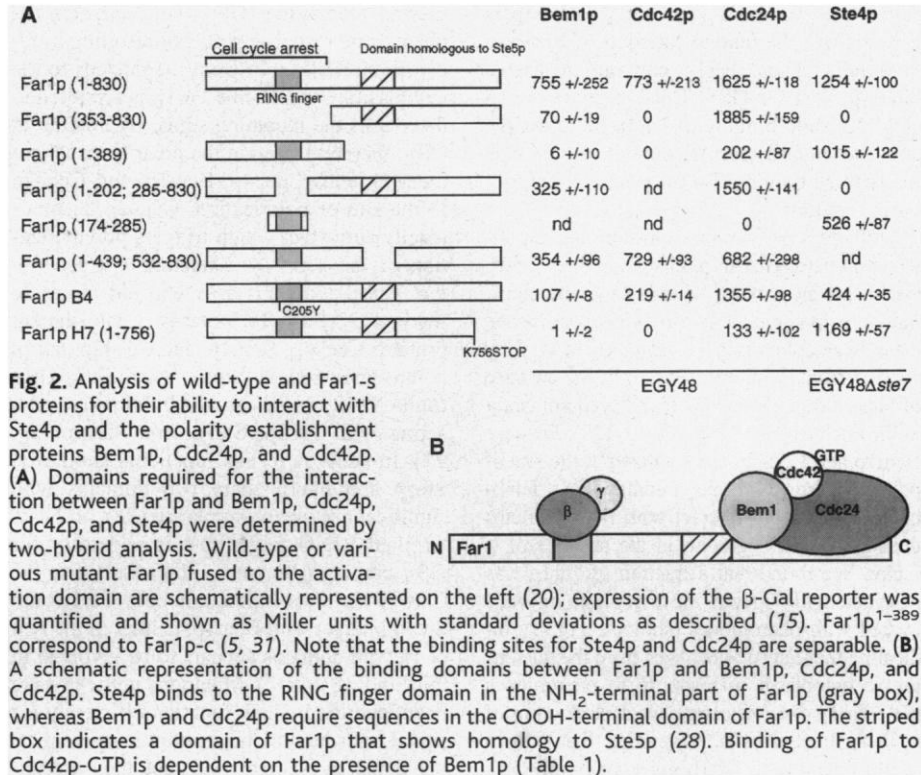


Fig. 2. Analysis of wild-type and Far1-s proteins for their ability to interact with Ste4p and the polarity establishment proteins Bem1p, Cdc42p, and Cdc24p. (A) Domains required for the interaction between Far1p and Bem1p, Cdc24p, Cdc42p, and Ste4p were determined by two-hybrid analysis. Wild-type or various mutant Far1p fused to the activation domain are schematically represented on the left (20); expression of the β-Gal reporter was quantified and shown as Miller units with standard deviations as described (15). Far1p¹⁻³⁸⁹ correspond to Far1p-c (5, 31). Note that the binding sites for Ste4p and Cdc24p are separable. (B) A schematic representation of the binding domains between Far1p and Bem1p, Cdc24p, and Cdc42p. Ste4p binds to the RING finger domain in the NH₂-terminal part of Far1p (gray box), whereas Bem1p and Cdc24p require sequences in the COOH-terminal domain of Far1p. The striped box indicates a domain of Far1p that shows homology to Ste5p (28). Binding of Far1p to Cdc42p-GTP is dependent on the presence of Bem1p (Table 1).

Fig. 1. Far1p interacts with the polarity establishment proteins Bem1p, Cdc42p, and Cdc24p, as well as Ste4p, the β subunit of the heterotrimeric G protein. (A) Complex formation between Far1p and Bem1p in vitro (16). Far1p tagged with two copies of the polyoma epitope (PT-Far1p; lanes 1 and 2) or with an HA-epitope as a control (HA-Far1p; lane 3) was purified from cells which were either treated (+; lanes 2 and 3) or not treated (-; lane 1) with α factor and incubated with 6His-tagged Bem1p purified from *E. coli*. Bound proteins were eluted with polyoma peptide and subjected to immunoblot analysis with antibodies specific for Bem1p (12). (B) Far1p interacts with Cdc24p in vivo. HA-tagged Cdc24p (lanes 2 and 3) or untagged Cdc24p as a control (lane 1) was immunoprecipitated with Δ*far1* antibodies from extracts prepared from Δ*far1* cells, which express Far1p from the inducible GAL promoter (17). Expression of Far1p was induced by addition of galactose (+) or repressed by the addition of glucose (-). Immunoprecipitates were blotted with polyclonal antibodies against Far1p (upper panel) or Cdc24p (lower panel). The bracket marks the position of Far1p; the arrow points to the position of HA-Cdc24p. (C) Far1p interacts with Ste4p in vivo. Extracts prepared from cells expressing Ste4p tagged with an HA-epitope (lanes 1 and 2) or untagged Ste4p as a control (lanes 3 and 4) were incubated with antibodies to HA, and the immunoprecipitates were analyzed for the presence of bound Far1p (upper panel) or Ste4p (lower panel) by immunoblotting with polyclonal antibodies. Extracts prepared from cells lacking Far1p (lane 5) or Ste4p (lane 6) confirm the specificity of the antibodies. Note that *ste4Δ* cells express low amounts of Far1p, because basal levels of Far1p depend on a functional signaling pathway (31). SN, soluble extract prior to immunoprecipitation; IP, immunoprecipitate with HA11 antibodies. The arrow points to the position of Far1p; the brackets mark the different forms of HA-Ste4p or untagged Ste4p. The asterisk marks the position of immunoglobulin G. (D) Far1p is specifically required for the interaction between Ste4p and Cdc24p. The interaction between Cdc24p and Ste4p was measured in different two-hybrid strains (14, 15). Bars show mean β-galactosidase activity ± SD for four independent transformants. Plasmids were pBTM-CDC24 (DBD-Cdc24), pGADXP (vector), pGAD-STE4 (AD-Ste4, low expression), and pGADXP-STE4 (AD-Ste4, high expression) (14). (E) Far1p and Cdc24p function in a common pathway during cellular orientation (19). *far1-c* or *cdc24-m* single mutants mate with comparable efficiency to *far1-c cdc24-m* double mutants, suggesting that the two mutant proteins are defective in the same cellular function. In contrast, *far1-c pea2-2* cells are synthetic sterile (5).

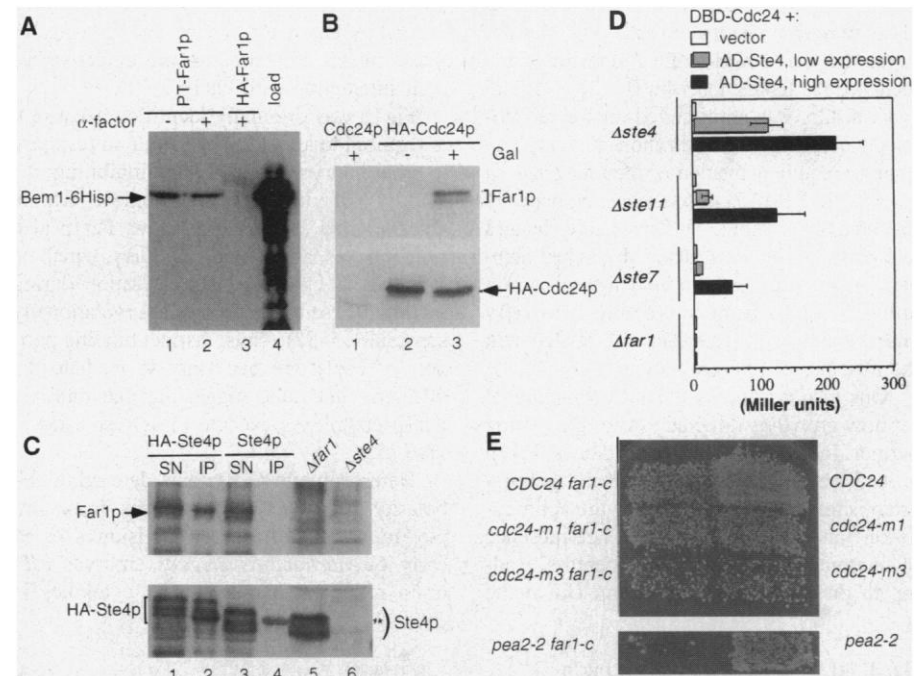


Fig. 1. Far1p interacts with the polarity establishment proteins Bem1p, Cdc42p, and Cdc24p, as well as Ste4p, the β subunit of the heterotrimeric G protein. (A) Complex formation between Far1p and Bem1p in vitro (16). Far1p tagged with two copies of the polyoma epitope (PT-Far1p; lanes 1 and 2) or with an HA-epitope as a control (HA-Far1p; lane 3) was purified from cells which were either treated (+; lanes 2 and 3) or not treated (-; lane 1) with α factor and incubated with 6His-tagged Bem1p purified from *E. coli*. Bound proteins were eluted with polyoma peptide and subjected to immunoblot analysis with antibodies specific for Bem1p (12). (B) Far1p interacts with Cdc24p in vivo. HA-tagged Cdc24p (lanes 2 and 3) or untagged Cdc24p as a control (lane 1) was immunoprecipitated with Δ*far1* antibodies from extracts prepared from Δ*far1* cells, which express Far1p from the inducible GAL promoter (17). Expression of Far1p was induced by addition of galactose (+) or repressed by the addition of glucose (-). Immunoprecipitates were blotted with polyclonal antibodies against Far1p (upper panel) or Cdc24p (lower panel). The bracket marks the position of Far1p; the arrow points to the position of HA-Cdc24p. (C) Far1p interacts with Ste4p in vivo. Extracts prepared from cells expressing Ste4p tagged with an HA-epitope (lanes 1 and 2) or untagged Ste4p as a control (lanes 3 and 4) were incubated with antibodies to HA, and the immunoprecipitates were analyzed for the presence of bound Far1p (upper panel) or Ste4p (lower panel) by immunoblotting with polyclonal antibodies. Extracts prepared from cells lacking Far1p (lane 5) or Ste4p (lane 6) confirm the specificity of the antibodies. Note that *ste4Δ* cells express low amounts of Far1p, because basal levels of Far1p depend on a functional signaling pathway (31). SN, soluble extract prior to immunoprecipitation; IP, immunoprecipitate with HA11 antibodies. The arrow points to the position of Far1p; the brackets mark the different forms of HA-Ste4p or untagged Ste4p. The asterisk marks the position of immunoglobulin G. (D) Far1p is specifically required for the interaction between Ste4p and Cdc24p. The interaction between Cdc24p and Ste4p was measured in different two-hybrid strains (14, 15). Bars show mean β-galactosidase activity ± SD for four independent transformants. Plasmids were pBTM-CDC24 (DBD-Cdc24), pGADXP (vector), pGAD-STE4 (AD-Ste4, low expression), and pGADXP-STE4 (AD-Ste4, high expression) (14). (E) Far1p and Cdc24p function in a common pathway during cellular orientation (19). *far1-c* or *cdc24-m* single mutants mate with comparable efficiency to *far1-c cdc24-m* double mutants, suggesting that the two mutant proteins are defective in the same cellular function. In contrast, *far1-c pea2-2* cells are synthetic sterile (5).

suggesting that binding of Gβγ to Far1p is essential for the mating function of Far1p in vivo (21). Thus, Far1p contains separable binding sites for Gβγ, Cdc24p, and Bem1p (Fig. 2B), and binding of Far1p to both Gβγ and the polarity establishment proteins is likely to be required for oriented cell polarity during mating.

Although pheromones did not alter the interaction between Far1p, Gβγ, and the polarity establishment proteins when assayed by coimmunoprecipitation or two-hybrid experiments, these interactions may be regulated in vivo by compartmentalization of Far1p. In the absence of pheromone, Far1p was found predominantly in the nucleus of G₁ cells (Fig. 3) (22). Because Bem1p and Cdc42p are localized at the site of polarized growth during budding (23), Far1p may be unable to interact with these proteins during vegetative growth in the absence of α factor. We found that a fraction of Far1p was distributed throughout the cytoplasm in cells treated with pheromones (shmoo; Fig. 3), indicating that Far1p relocates from the nucleus to the cytoplasm in response to pheromones (24). Far1p did not accumulate at shmoo tips of α factor-treated cells, suggesting that only a small fraction of Far1p interacts with Gβγ or that its interaction with Gβγ might be transient. Like wild-type Far1p, truncated Far1¹⁻³⁸⁹ protein was localized to the cytoplasm in pheromone-treated cells (Fig. 3), indicating that the COOH-terminal domain, which mediated the interaction with Bem1p, Cdc24p, and Cdc42p, was not required for the redistribution of Far1p. Relocalization of Far1p appears to require activation of the mitogen-activated protein (MAP) kinase signaling pathway triggered by α factor (25). Thus, Far1p changes its localization in an α factor-dependent manner, suggesting that compartmentalization prevents Far1p from interacting with Gβγ and the polarity establishment proteins in the absence of pheromones.

Our results support the following model for how growth is directed toward the mating partner. In the absence of pheromones, Far1p is localized in the nucleus, and the polarity establishment proteins organize the actin cytoskeleton toward the bud site. The presence of pheromones activates the receptors, leading to dissociation of Gβγ from Gα at the

plasma membrane. Gβγ then activates the pheromone response pathway resulting in redistribution of Far1p from the nucleus to the cytoplasm. Cytoplasmic Far1p is recruited to the site of the incoming signal by binding to Gβγ, thereby targeting the polarity establishment proteins Cdc24p, Bem1p, and Cdc42p to the site of polarization. Cdc42p becomes locally activated, which triggers polymerization of the actin cytoskeleton. We propose that Far1p functions as a scaffold molecule linking Gβγ to the polarity establishment proteins Cdc24p, Bem1p, and Cdc42p. Far1p is thus analogous to Ste5p, which links Gβγ to the MAP kinase cascade by directly interacting with Fus3p, Ste7p, and Ste11p (26, 27). In addition to this functional similarity, Ste5p and Far1p share two domains with significant sequence similarity (28): an NH₂-terminal RING finger that is necessary for Gβγ binding (29), and a short stretch in the COOH-terminus. Although both Far1p and Ste5p interact with Bem1p, neither of the two conserved domains appears to be involved in this binding (Fig. 2). Mutations in Ste4p have been identified which function efficiently for signal transduction, but exhibit a severe mating defect presumably because they are unable to orient cell polarity toward the mating partner (30), suggesting that specific Ste4p mutations may be able to distinguish between several effectors. It is not known whether these mutant Ste4 proteins are defective for their interaction with Far1p.

Far1p was originally identified because it is required to arrest the cell cycle in response to pheromones, probably by inhibiting the activity of the cyclin-dependent kinase Cdc28p-Clnp (31). As we show, Far1p also functions as an effector of Gβγ which is involved in cytoskeletal polarization during mating. These two activities are mutationally separable (5, 32). Thus, distinct binding partners of Far1p are necessary to mediate the different functions, suggesting that multiple Far1p complexes execute these responses in vivo (5).

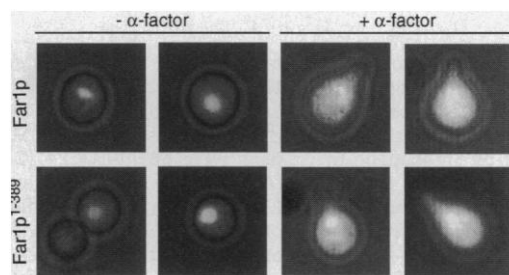
Heterotrimeric G proteins determine cell polarity in a variety of organisms, for example, in orientation of cell division axes in early *Caenorhabditis elegans* embryos (32) or in response to chemotactic cytokines in

leukocytes (33). In *Drosophila melanogaster*, signaling mediated by the G protein-coupled receptor, Frizzled, polarizes precursor cells and specifies asymmetric cell divisions by properly orienting mitotic spindles (34). Although the effectors of the G proteins in these systems are not known, the domain of Cdc24p required to interact with Far1p is conserved in mammalian exchange factors such as the *DBL* proto-oncogene (6), suggesting that Far1p-like molecules may link G protein coupled receptor signaling pathways to polarized cell growth in all eukaryotes.

References and Notes

1. J. Chenevert, *Mol. Biol. Cell* **5**, 1169 (1994); D. G. Drubin and W. J. Nelson, *Cell* **84**, 335 (1996); J. Chant, *Curr. Opin. Cell Biol.* **8**, 557 (1996); L. Van Aelst and C. D'Souza-Schoorey, *Genes Dev.* **11**, 2295 (1997); A. Hall, *Science* **279**, 509 (1998).
2. I. Herskowitz, *Cell* **80**, 187 (1995); E. Leberer, D. Y. Thomas, M. Whiteway, *Curr. Opin. Genet. Dev.* **7**, 59 (1997); G. F. Sprague and J. W. Thorner, in *The Molecular and Cellular Biology of the Yeast Saccharomyces*, E. W. Jones, J. R. Pringle, J. R. Broach, Eds. (Cold Spring Harbor Laboratory Press, Cold Spring Harbor, NY, 1992), p. 657.
3. H. R. Bourne, *Curr. Opin. Cell Biol.* **9**, 134 (1997); H. E. Hamm, *J. Biol. Chem.* **273**, 669 (1998); D. E. Clapham and E. J. Neer, *Annu. Rev. Pharmacol. Toxicol.* **37**, 167 (1997); H. E. Hamm and A. Gilchrist, *Curr. Opin. Cell Biol.* **8**, 189 (1996).
4. J. E. Segall, *Proc. Natl. Acad. Sci. U.S.A.* **90**, 8332 (1993).
5. J. Chenevert, N. Valtz, I. Herskowitz, *Genetics* **136**, 1287 (1994); N. Valtz, M. Peter, I. Herskowitz, *J. Cell Biol.* **131**, 863 (1995); R. Dorer, P. M. Pryciak, L. H. Hartwell, *ibid.*, p. 845.
6. A. Nern and R. A. Arkowitz, *Nature* **391**, 195 (1998).
7. K. Schrick, B. Garvik, L. H. Hartwell, *Genetics* **147**, 19 (1997).
8. J. L. Brown, M. Jaquenoud, M. P. Gulli, J. Chant, M. Peter, *Genes Dev.* **11**, 2972 (1997); G. C. Chen, Y. J. Kim, C. S. Chan, *ibid.*, p. 2958.
9. B. F. Sloat and J. R. Pringle, *Science* **200**, 1171 (1978); Y. Zheng, R. Cerlone, A. Bender, *J. Biol. Chem.* **269**, 2369 (1994).
10. J. Peterson *et al.*, *J. Cell Biol.* **127**, 1395 (1994).
11. H.-O. Park, E. Bi, J. R. Pringle, I. Herskowitz, *Proc. Natl. Acad. Sci. U.S.A.* **94**, 4463 (1997).
12. T. Leeuw *et al.*, *Science* **270**, 1210 (1995).
13. D. M. Lyons, S. K. Mahanty, K. Y. Choi, M. Manandhar, E. A. Elion, *Mol. Cell Biol.* **16**, 4095 (1996).
14. Unless noted otherwise two-hybrid assays were performed using pEG202-based plasmids expressing LexA DNA-binding domain fusions (DBD), and pJG4-5-based plasmids containing fusions to the B42 transcriptional activation domain (AD) (35). pEG203 and pJG4-6 are derivatives of pEG202 and pJG4-5, respectively, with an altered polylinker (kind gift of E. O'Shea). The FAR1 coding sequence was amplified by polymerase chain reaction (PCR) using the primers oTP410 and oTP404, digested with Nco I and Xho I, and ligated into pJG4-6 to yield ACB412. The sequences of all primers used in this study are available as supplementary material at www.sciencemag.org/feature/data/983067.shl. The coding sequence of wild-type CDC24 or CDC24-M alleles (6) was amplified by PCR using the primers oTP474 and oTP464, digested with Eco RI and Xho I, and ligated into pEG202. Plasmid pKP1, which allows expression of an NH₂-terminally truncated Cdc24p (amino acids 283 to 853) fused to the LexA DNA-binding domain, was constructed by ligating the genomic 2300-base pair (bp) Eco RI-Bam HI fragment of CDC24 into pEG202. pBTM-CDC24 (2 μm, TRP1, lexA DBD-CDC24) contains full-length, PCR-amplified CDC24 inserted into pBTM116 (36) as a Bam HI-Pst I fragment. The two-hybrid plasmids carrying STE4 were generated

Fig. 3. Far1p relocates from the nucleus to the cytoplasm in response to pheromones. Cells expressing either full-length Far1p (upper row) or Far1p¹⁻³⁸⁹ (Far1p-c, lower row) fused to GFP were treated (right panels, +) or not treated (left panels, -) with α factor. No staining was detected in cells expressing untagged Far1p (47). Photographs show GFP fluorescence overlaid with the corresponding phase contrast image. Note that Far1p is nuclear in G₁ cells in the absence of α factor but accumulates in the cytoplasm of cells treated with α factor.



- by PCR and cloned into pEG202 for the LexA DNA binding domain fusion (pLH163) or pJG4-5 for the B42 transcriptional activation domain fusion (pLH119). pGAD-STE4 (2 μ m, *LEU2*, truncated *ADH1* promoter, *GAL4 AD-STE4*) containing full-length Ste4p in pGAD424 has been described previously [P. M. Pryciak and L. H. Hartwell, *Mol. Cell Biol.* **16**, 2614 (1996)]. pGADXP (2 μ m, *LEU2*, full-length *ADH1* promoter, *GAL4 AD-STE4*) was constructed by replacing the GAD/polylinker-containing Hind III fragment of pGAD GH (Clontech) with the analogous Hind III fragment from pGAD424 (Clontech); differences in *ADH1* promoter length in pGAD424 and pGAD GH result in different expression levels of the AD-fusions. pGADXP-STE4 (2 μ m, *LEU2*, full-length *ADH1* promoter, *GAL4 AD-STE4*) contains full-length, PCR-amplified *STE4* inserted into pGADXP as an Eco RI-Bam HI fragment. The two-hybrid plasmids for Bem1p, Gic2p, Cdc42p, Rho1p, and Ste18p have been described previously (8). LexA-fusions to Cdc42p and Rho1p contain the COOH-terminal Cys-to-Ser substitutions to prevent prenylation.
15. Two-hybrid assays were performed in yeast strain EGY48 (35) or L40 (36). Strains YACB167 (*far1 Δ ::LEU2*), LH64 (*ste7 Δ ::hisG*), YACB39 (*bem1 Δ ::LEU2*), YACB168 (*ste4 Δ ::LEU2*) are derivatives of EGY48 and were constructed by one-step gene replacement (37) using the plasmids pTP428, pLH126, pTP154, and pTP516, respectively (5, 21). Two-hybrid tester strains PPY758 (*ste4 Δ*), PPY762 (*ste11 Δ*), PPY746 (*ste7 Δ*), and PPY760 (*far1 Δ*), are derivatives of strain L40 in which the indicated genes were disrupted using *ADE2*-marked replacement constructs pSL2199, pSL2222, pSL2270, and pSL2200, respectively (27). Standard yeast growth conditions were used as described [C. Guthrie and G. R. Fink, *Guide to Yeast Genetics and Molecular Biology* (Academic Press, San Diego, CA, 1991)]. Yeast transformations were performed by the lithium acetate method [H. Ito, Y. Fukuda, K. Murata, A. Kimura, *J. Bacteriol.* **153**, 163 (1983)]. *LacZ* reporter activity was measured as described previously (8); averages and standard deviations were determined from at least three independent experiments. When possible, two-hybrid interactions were confirmed with both DNA- and activation domain fusions. In Fig. 2A, un-specific Miller units determined with cells transformed with control plasmid pRFHM1 (35) and the activation domain fusion as well as an empty plasmid (pJG4-5 or pJG4-6) and fusions to the DNA binding domain were subtracted from specific Miller units obtained with cells carrying plasmids expressing fusions to both tested proteins. The interaction between Far1p and Cdc24p was similar in strains deleted for *STE4* (YACB168), *STE11* (PPY762) or *STE7* (PPY746), and thus was not dependent on Ste4p or activity of the pheromone response pathway. Similarly, deletion of *FAR1* (PPY760) did not affect interactions between Ste4p and the Ste4p-targets Gpa1p, Ste18p, Ste5p NH₂-terminus, and Akr1p. No significant differences in *LacZ* reporter activity were detected when two-hybrid assays with Far1p and Bem1p or Cdc24p were performed with cells treated or not treated with α factor.
 16. Purification of Far1p tagged with two copies of the polyoma tag (PT) was performed essentially as described (38). Briefly, strain K2180 (*MATa ade2-1 trp1-1 can1-100 leu2-3,112 his3-11,15 ura3 far1::hisG bar1::hisG GAL⁺ ssd1-d2*) was transformed with plasmids expressing PT-Far1p (pTP523) or HA-Far1p (pTP90), respectively, and grown to early log phase in selective medium containing 2% galactose. Where indicated, α factor to 10⁻⁶ M was added for 2 hours. Cells were harvested by centrifugation, resuspended in buffer TNE450 [50 mM Tris-HCl (pH 7.5), 450 mM NaCl, 10 mM EDTA, and 0.1% NP-40] and broken with glass beads in a Mini Beadbeater (Biospec). After two sequential centrifugations, the supernatant was incubated for 1 hour with protein G-sepharose beads (Pharmacia) covalently coupled to polyoma antibodies (39). Beads were washed three times with buffer TNE450 and twice with binding buffer [10 mM Tris-HCl (pH 7.5), 85 mM NaCl, 10 mM EDTA, 0.1% NP-40]. The beads were then divided into aliquots and incubated for 30 min at 4°C with Bem1p-6His purified from *E. coli* (17). The beads were washed three times with binding buffer and Far1p was then specifically eluted with binding buffer containing 10 μ M polyoma peptide (EYMPME) and 0.1% *N*-octylglucoside (Fluka). Bound Bem1p-6His was detected by immunoblotting using polyclonal antibodies against Bem1p (12).
 17. YMP290 cells (*MATa ade2-1 trp1-1 can1-100 leu2-3,112 his3-11,15 ura3 GAL⁺ psi⁺ ssd1-d2 bar1-1 Δ far1*) were transformed with a plasmid expressing epitope-tagged HA-Cdc24p or for control untagged Cdc24p from the *ADH*-promoter and a plasmid expressing Far1p from the inducible *GAL* promoter (40). Cells were grown in selective media containing raffinose (2% final concentration) to early log phase, at which time galactose (2% final concentration; indicated by "+" in Fig. 1B) or for control glucose (2% final concentration; indicated by "-") was added for 5.5 hours at 30°C to regulate expression of Far1p. α factor was added at 1 μ g/ml final concentration and incubated for 90 min. Cells were pelleted, resuspended in RIPA buffer [50 mM Tris (pH 7.5), 50 mM NaCl, 1% NP40, 0.5% deoxycholate, 0.1% SDS, 20 mM β -glycerophosphate, 50 mM NaF, 1 mM Na₃VO₄] containing the protease inhibitors PMSF, aprotinin, leupeptin, and pepstatin, and lysed with glass beads using a bead beater (BioSpec). The soluble extract was then incubated for two hours at 4°C with sepharose beads coupled to HA11 monoclonal antibodies (BabCO). The beads were washed four times with RIPA buffer and twice with phosphate buffered saline (PBS) [137 mM NaCl, 2.7 mM KCl, 4.3 mM Na₂HPO₄·7H₂O, 1.4 mM KH₂PO₄ (pH 7.3)]. Bound proteins were eluted with gel-sample buffer and subjected to immunoblot analysis with polyclonal antibodies against Far1p and Cdc24p. Polyclonal antibodies against Cdc24p were raised against a MalE-Cdc24 fusion protein (kindly provided by E. Bi) and affinity purified as described (39). Coimmunoprecipitation experiments with Far1p and Ste4p were carried out as above, except that YMP290 cells were transformed with plasmids expressing Far1p (ACB435) (40) and either epitope-tagged HA-Ste4p (pYEE181) (13) or untagged Ste4p (pTP288) from the inducible *GAL* promoter. HA11-immunoprecipitates were immunoblotted with polyclonal antibodies against Far1p and Ste4p.
 18. Z. S. Zhao, T. Leung, E. Manser, L. Lim, *Mol. Cell Biol.* **15**, 5246 (1995).
 19. Strains YACB175 (*far1-c*), YACB176 (*far1-c cdc24-m1*) and YACB178 (*far1-c cdc24-m3*) are derivatives of RAY914 (6), whereas strains YMP487 (*pea2-2*) and YACB183 (*pea2-2 far1-c*) are derivatives of IH2627 (5). *far1-c* is a mating specific *far1-s* allele which expresses a truncated Far1p lacking the COOH domain (Far1p¹⁻³⁸⁹). All strains were constructed by single-step gene replacement (37) using the plasmid pTP4 digested with Not I (37); successful replacement of the endogenous *FAR1* locus by *far1-c* was confirmed by the appearance of truncated Far1-c protein by immunoblotting. Mating assays were carried out with the mating tester IH1793 as described (21). In contrast to double mutants between *far1-c* and proteins functioning in the default mating pathway (such as Pea2p) (5), *far1-c cdc24-m* double mutants mate with an efficiency comparable to each single mutant.
 20. The set of Far1p-deletion constructs in the two-hybrid vector pJG4-6 was constructed by PCR using pTP62 (22) as template and the primer pairs oTP418/oTP404, oTP410/oTP411, and oTP328/oTP329, all of which contain Nco I or Not I and Xho I restriction sites, respectively. The sequences of all primers used in this study are available at www.sciencemag.org/feature/data/983067.shl. The PCR fragments were purified, digested with Nco I or Not I and Xho I, and ligated into pJG4-6. The resulting plasmids are referred to as ACB418 (Far1p³⁵³⁻⁸³⁰), ACB413 (Far1p¹⁻³⁸⁹) and ACB415 (Far1p¹⁷⁴⁻²⁸⁵). Far1p¹⁻³⁸⁹ corresponds to Far1p-c (31). The PCR fragment amplified with the primer pair oTP418/oTP404 digested with Not I and Xho I was also ligated into pEG203 to yield plasmid ACB414. Constructs lacking the RING finger domain (amino acids 203 to 284) or the Ste5p homology domain (amino acids 440 to 531) were constructed by site-directed mutagenesis using the ExSite kit as recommended by the manufacturer (Stratagene); the introduced mutations were confirmed by sequencing. The fragments were cloned into pJG4-6 for two-hybrid analysis (generating plasmids pTP524 and ACB421) or pRD53 (generating plasmids pTP525 and pKP7) for mating assays. Genomic DNA isolated from strains IH2640 and IH2637 (5) was used to amplify the coding sequences of the *far1-s* alleles H7 and B4 by PCR using the primers oTP410 and oTP404. The obtained fragments were digested with Nco I and Xho I and ligated into pJG4-6 for two-hybrid analysis to generate plasmids ACB425 and ACB426. Expression of all Far1 mutants and fusion proteins was controlled by immunoblotting with Far1p-specific antibodies.
 21. Mating and orientation assays were performed using the mating testers IH2625 (*MATa lys1 far1-c*) and IH1793 (*MATa lys1*) as described (38). Cells deleted for *FAR1* (YMP290) (17) were transformed with plasmids expressing mating-specific alleles either from the endogenous or the *GAL* promoter. All truncated *FAR1* alleles shown in Fig. 2 are unable to perform the mating function of Far1p. Cells harboring *FAR1^{1-203/284-830}* are able to arrest the cell cycle but mated like vector controls at 1% of the wild-type levels, demonstrating that the RING finger is required for the mating function of Far1p. The cells were unable to orient towards the mating partner, as determined by confusion assays (1.5-fold inhibition of the mating efficiency in the presence of excess amounts of α factor, in contrast to 85-fold inhibition of wild-type cells) and quantitative analysis of the position of bud scars with respect to the shmoo site in zygotes (81% of the remaining zygotes have bud scars adjacent to the mating partner, in contrast to 18% in wild-type cells). Shmoo morphology was examined after addition of 10⁻⁶ M α factor to 3 ml of log phase cultures at 30°C. Cells were sonicated, fixed with formaldehyde to a final concentration of 3.7%, and viewed by differential interference microscopy. Yeast actin was visualized with rhodamine-phalloidin (Molecular Probes, Eugene, OR) as described previously [M. Peter, A. M. Neiman, H.-O. Park, M. van Lohuizen, I. Herskowitz, *EMBO J.* **15**, 7046 (1996)].
 22. S. Henchoz et al., *Genes Dev.* **11**, 3046 (1997).
 23. M. Ziman et al., *Mol. Biol. Cell* **4**, 1307 (1993); K. R. Ayscough et al., *J. Cell Biol.* **137**, 399 (1997); J. R. Pringle et al., *Cold Spring Harbor Symp. Quant. Biol.* **60**, 729 (1995).
 24. The plasmid pTP68 expressing functional full-length Far1p-green fluorescent protein (GFP) has been described previously (22). A fragment coding for the NH₂-terminal 389 amino acids of Far1p was amplified by PCR using the primers oTP330 and oTP331, digested with Xho I and Eco RI and ligated in a three-fragment ligation with the Eco RI-Bam HI fragment encoding GFP-S65T [R. Heim, A. B. Cubitt, R. Y. Tsien, *Nature* **373**, 663 (1995)] and the vector pRD53 linearized with Xho I and Bam HI, to yield plasmid pTP76. YMP290 (*MATa ade2-1 trp1-1 can1-100 leu2-3,112 his3-11,15 ura3 GAL⁺ psi⁺ ssd1-d2 bar1-1 Δ far1*) was transformed with plasmids pTP68 (Far1p-GFP), pTP76 (Far1p¹⁻³⁸⁹-GFP) or for control pRD53, and cells were grown in selective medium containing 2% galactose. Where indicated, 10⁻⁶ M α factor was added for 2 hours. Immunoblots with Far1p antibody confirmed that full-length Far1p-GFP and Far1p¹⁻³⁸⁹-GFP expressed from the *GAL* promoter were present at similar levels in cells treated or not treated with α factor. GFP fluorescence was visualized on a Zeiss Axiovert 100 microscope equipped with a Chroma GFP filter (excitation at 470 to 440 nm wavelength) and photographed with a Photometrics CCD (charge-coupled device) camera as described [M. Jaquenoud, M.-P. Gulli, K. Peter, M. Peter, *EMBO J.* **17**, 5360 (1998)]. Immunofluorescence experiments using Far1p fused to three copies of the myc epitope confirmed that, in the absence of pheromones, Far1p is localized in the nucleus, whereas in pheromone treated cells, Far1p is found predominantly in the cytosol.
 25. M. Blondel and M. Peter, unpublished results.
 26. K. Y. Choi, B. Satterberg, D. M. Lyons, E. A. Elion, *Cell* **78**, 499 (1994); S. Marcus, A. Polverino, M. Barr, M. Wigler, *Proc. Natl. Acad. Sci. U.S.A.* **91**, 7762 (1994).

27. J. A. Printen and G. F. Sprague Jr., *Genetics* **138**, 609 (1994).
 28. E. A. Elion, *Trends Cell Biol.* **5**, 322 (1995); E. Leberer et al., *Mol. Gen. Genet.* **241**, 241 (1993).
 29. M. S. Whiteway et al., *Science* **269**, 1572 (1995); C. Inouye, N. Dhillon, J. Thorner, *ibid.* **278**, 103 (1997); Y. Feng, L. Y. Song, E. Kincaid, S. K. Mahanty, E. A. Elion, *Curr. Biol.* **8**, 267 (1998); P. M. Pryciak and F. A. Huntress, *Genes Dev.* **12**, 2684 (1998).
 30. L. S. Huang and I. Herskowitz, unpublished results.
 31. F. Chang and I. Herskowitz, *Cell* **63**, 999 (1990); M. Peter, A. Gartner, J. Horecka, G. Ammerer, I. Herskowitz, *ibid.* **73**, 747 (1993); M. Peter and I. Herskowitz, *Science* **265**, 1228 (1994); A. Gartner et al., *Mol. Cell Biol.* **18**, 3681 (1998).
 32. R. R. Zwaal et al., *Cell* **86**, 619 (1996).
 33. C. A. Parent, B. J. Blacklock, W. M. Froehlich, D. B. Murphy, P. N. Devreotes, *ibid.* **95**, 81 (1998); S. G. Ward, K. Bacon, J. Westwick, *Immunity* **9**, 1 (1998).
 34. P. N. Adler, R. E. Krasnow, J. Liu, *Curr. Biol.* **7**, 940 (1997); M. Gho, F. Schweisguth, *Nature* **393**, 178 (1998); D. I. Strutt, U. Weber, M. Mlodzik, *ibid.* **387**, 292 (1997).
 35. J. Gyuris, E. Golemis, H. Chertkov, R. Brent, *Cell* **75**, 791 (1993).
 36. S. M. Hollenberg et al., *Mol. Cell Biol.* **15**, 3813 (1995).
 37. R. Rothstein, *Methods Enzymol.* **194**, 281 (1991).
 38. N. Valtz and M. Peter, *ibid.* **283**, 350 (1997).
 39. E. Harlow and D. Lane, *Antibodies: A Laboratory Manual* (Cold Spring Harbor Laboratory Press, Cold Spring Harbor, NY, 1988).
 40. The plasmid ACB435 expressing full-length Far1p from the GAL promoter was constructed as follows: plasmid pTP62 (22) was digested with Bam HI, the 1910-bp fragment was purified and ligated together with the 582 bp Bam HI-Xho I fragment isolated from plasmid ACB414 (20) into pRS315(G) [R. S. Sikorski and P. Hieter, *Genetics* **122**, 19 (1989)] linearized with Bam HI and Xho I. Expression of the Far1 protein was controlled by immunoblotting with Far1p antibodies. A single copy of the HA epitope was fused to the NH₂-terminus of CDC24 using PCR, and the fragment was cloned into the vector p425(ADH) [D. Mumberg, R. Müller, M. Funk, *Gene* **156**, 119 (1995)], which allows expression of Cdc24p

from the constitutive ADH promoter. The plasmid fully restores viability of a temperature-sensitive cdc24-5 strain at 37°C.
 41. A.-C. Butty and M. Peter, data not shown.
 42. We thank members of each laboratory for helpful discussions; C. Boone, R. A. Arkowitz, J. Chant, D. Lew, M. Funk, E. Elion, E. O'Shea, H.-O. Park, E. Bi, and E. Leberer for plasmids and strains; B. Catarin for polyclonal antibodies to Far1p; and E. Leberer for antibodies to Bem1p. We also thank N. Valtz, S. Henchoz and K. Peter for help during early aspects of this work and J. Phillips, V. Simanis, and R. Iggo for critical reading of the manuscript. L.S.H. was supported by an NIH postdoctoral fellowship. Work in the I.H. laboratory was supported by an NIH research grant (GM48052). P.M.P. is supported by grants from the Worcester Foundation, the Millipore Foundation, and NIH (GM57769). M.P. is supported by the Swiss National Science Foundation, the Swiss Cancer League, and a Helmut Horten Incentive award. I.H. dedicates this paper to J. Stahl.

9 June 1998; accepted 16 October 1998

Localization of Bacterial DNA Polymerase: Evidence for a Factory Model of Replication

Katherine P. Lemon and Alan D. Grossman*

Two general models have been proposed for DNA replication. In one model, DNA polymerase moves along the DNA (like a train on a track); in the other model, the polymerase is stationary (like a factory), and DNA is pulled through. To distinguish between these models, we visualized DNA polymerase of the bacterium *Bacillus subtilis* in living cells by the creation of a fusion protein containing the catalytic subunit (PolC) and green fluorescent protein (GFP). PolC-GFP was localized at discrete intracellular positions, predominantly at or near midcell, rather than being distributed randomly. These results suggest that the polymerase is anchored in place and thus support the model in which the DNA template moves through the polymerase.

For all organisms, the production of viable progeny depends on the faithful replication of DNA by DNA polymerase. A conceptual question about in vivo DNA replication remains unsettled. During replication, does the DNA polymerase move along the DNA template? or is the DNA polymerase in a fixed position with the DNA template moving through the replication machinery? Studies with eukaryotic cells have indicated that DNA replication proteins and newly replicated DNA are present at numerous discrete foci [so-called replication factories (1)], resulting in the hypothesis that DNA replication occurs at fixed locations. However, analysis of eukaryotic DNA polymerase is complicated because replication starts from many different origins and because it is difficult to orient the foci within the eukaryotic nucleus.

Like many bacteria, *Bacillus subtilis* has a single circular chromosome [~4200 kilobase pairs (2)], and DNA replication initiates from a single origin (*oriC*) and proceeds bidirectionally (3). Most of the proteins present at the replication fork are conserved in prokaryotes and eukaryotes (4).

We attempted to determine whether, in a population of cells at different stages of the replication cycle, the replicative DNA polymerase of *B. subtilis* functions at fixed intra-

cellular positions or if it is randomly distributed along the nucleoid. We visualized DNA polymerase in living cells using a fusion protein consisting of the catalytic subunit (PolC) attached in-frame to green fluorescent protein (GFP). *polC-gfp* was placed in single copy in the *B. subtilis* chromosome under control of the endogenous *polC* promoter (5). PolC-GFP supported DNA replication and cell growth when it was present as the only source of the catalytic subunit, and it was visible as discrete fluorescent foci, at or near midcell, in most cells during exponential growth (Fig. 1A) (6). In these cells, the DNA occupied most of the cytoplasmic space and appeared to extend to the cell boundaries (Fig. 1B).

Two experimental observations indicated that the foci correspond to DNA polymerase at replication forks: (i) the presence of foci was dependent on continued DNA synthesis and (ii) the number of foci per cell increased at faster growth rates. We prevented reinitiation of DNA replication by inhibiting expression of DnaA, which binds to *oriC* and is required for assembly of the replication complex (3, 4). We fused *dnaA* to the LacI-repressible isopropyl-β-D-thiogalactopyranoside (IPTG)-inducible promoter Pspac (7) so that transcription of *dnaA* was IPTG-dependent. In the presence of IPTG (expression of *dnaA*), <5% of the cells lacked the visible

Table 1. The number of PolC-GFP foci per cell increased at faster growth rates. Cells were grown at 30°C in defined minimal medium (21) with the indicated carbon source (1%). All 20 amino acids (aa) were added in glucose + aa. Doubling times were rounded to the nearest 5 min, and samples were taken during exponential growth. In succinate, only one cell had three foci, and no cells had four. Six cells had five foci of PolC-GFP (three each from the glucose and glucose + aa cultures).

Doubling time (min)	Supplement	Total cells (n)	Cells with indicated number of foci (%)				
			0	1	2	3	4
230	Succinate	1317	24	56	19	0.08	<0.08
115	Glucose	635	3	43	41	9	3.6
75	Glucose + aa	454	2	33	32	22	10

Department of Biology, Building 68-530, Massachusetts Institute of Technology, Cambridge, MA 02139, USA.

*To whom correspondence should be addressed. E-mail: adg@mit.edu